









# Additives screening for the formulation of solid lipid nanoparticles of alpha-mangostin

Nagendra Babu VUTTI<sup>1</sup> , SN Koteswara Rao GUDHANTI<sup>2,3\*</sup> , Rajasekhar Reddy ALAVALA<sup>3</sup> ,  
Prasanna Kumar DESU<sup>1</sup> , Roja Rani BUDHA<sup>4</sup> , Kishore Babu GOVADA<sup>5</sup> , Durga Prasad ARJA<sup>5</sup> ,  
Nagendra CH<sup>5</sup> 

<sup>1</sup> College of Pharmacy, Koneru Lakshmaiah Education Foundation, Vaddeswaram, Andhra Pradesh 522502, India.

<sup>2</sup> Department of Pharmacy, School of Medical and Allied Sciences, Galgotias University, Greater Noida, Uttar Pradesh, 203201, India

<sup>3</sup> Shobhaben Pratapbhai Patel School of Pharmacy & Technology Management, SVKM's NMIMS, Vile Parle (W), Mumbai 400056, India.

<sup>4</sup> Department of Pharmacology, Institute of Pharmaceutical Technology, Sri Padmavathi Mahila Visvavidyalayam, Tirupati, A.P., 517502, India.

<sup>5</sup> Department of Formulation R&D, Laila Nutraceuticals, Vijayawada, Andhra Pradesh 520007, India.

\* Correspondence author. E-mail: drgsnkrao@gmail.com (GSN Koteswara Rao); Tel. +91-7989759439

Received: 12 July 2022 / Revised: 31 October 2022 / Accepted: 02 November 2022

**ABSTRACT:** The purpose of the study is to perform pre-formulation studies for alpha-mangostin ( $\alpha$ -mangostin) and screening of additives (such as solid lipids, emulsifiers and cryoprotectants) and their combinations (ratio of lipids, ratio of drug: lipid, ratio of emulsifier: co-emulsifier and concentration of cryoprotectant) used in the formulation of solid lipid nanoparticles of  $\alpha$ -mangostin. This screening is essential for the formulation of solid lipid nanoparticles (SLNP) that provide small particle size and PDI, high entrapment efficiency and zeta potential. This screening offers a rationale for selecting additives and their concentrations for formulating optimized SLNP. Pre-formulation studies showed melting point of 181.5°C, partition coefficient of 0.359 and drug solubility of 0.3072, 0.4576, 0.4892 and 0.5782 mg/mL in 1.2, 6.8, 7.0 and 7.5 pH buffers respectively. Ultimately, the DSC thermogram defines the sharp endotherm of  $\alpha$ -mangostin at 195.98°C. Hot melt homogenization followed by ultrasonication technique is used to develop solid lipid nanoparticles. Process parameters such as homogenization speed (15,000 rpm) and ultra sonication (6 minutes) was optimized based on particle size and PDI. The optimized formulation of SLNP of  $\alpha$ -mangostin contain 1:2:0.5:0.5:5 ratio of Drug: Solid lipid (0.8:1.2 ratio of Stearic acid: Preciol ATO5): Poloxamer 407: Sodium taurocholate: Mannitol.

**KEYWORDS:**  $\alpha$ -mangostin; Pre-formulation studies; Solid lipid nanoparticles; Additives screening.

## 1. INTRODUCTION

The tropical fruit tree mangosteen (*Garcinia mangostana*) has become a well-studied plant lead in the hunt for novel chemicals with interesting biological functions and possible medicinal uses [1]. Arthritis, diarrhoea, dysentery, inflammation, skin problems, and wounds have all been treated using the herb in the past [2]. Xanthone derivatives are the main bioactive chemicals in mangosteen fruits; more than 50 xanthones have been discovered from mangosteen pericarp [3]. The two principal xanthone derivatives in mangosteen extracts are  $\alpha$ - and  $\delta$ -mangostin, although the quantities of these compounds in such extracts vary depending on the extraction process [4–6]. *In-vitro* biological activities of mangosteen fruit extracts and pure chemicals include anti-oxidant [7, 8], anti-inflammatory [9], anti-bacterial [10], cytotoxic [11, 12], and cancer chemoprevention-related actions [13–15]. In the United States, the market for mangosteen dietary supplements has exploded, although there have been few scientific trials to prove their usefulness and safety. In obese participants, Udani et al. [16] observed probable anti-inflammatory effects from a commercial mangosteen juice combination. Kondo et al. [17] also found that ingesting another commercial

**How to cite this article:** Vatti NB, Gudhanti KR, Alavala RR, Desu PK, Budha RR, Govada KB, Arja DP, CH N. Additives screening for the formulation of solid lipid nanoparticles of alpha-mangostin. J Res Pharm. 2023; 27(2): 794-810.

mangosteen product improved anti-oxidant activity in healthy human participants. According to Li L et al.'s research, pure  $\alpha$ -mangostin has a minimal bioavailability in rats following oral administration [18]. According to a recent investigation,  $\alpha$ -mangostin was conjugated in the blood following oral administration of a mangosteen extract with known xanthone composition to human participants [19]. As the bioavailability of  $\alpha$ -mangostin is poor, formulating an SLNP will decrease the particle size and improve the bioavailability of  $\alpha$ -mangostin.

Solid lipid nanoparticles (SLNP) have lately received much interest as a possible alternative to liposomes and lipid-based emulsions for drug delivery. The use of solid lipids is an appealing innovation because the solid matrix of the lipid allows for more flexibility in drug release management and protects the encapsulated constituents from chemical degradation. Furthermore, SLNP have a slower *in-vivo* disintegration rate than liposomes due to their solid matrix. SLNP are physiological and biocompatible lipids that represent no acute or chronic toxicity concern. In addition, lipids have been employed in the manufacture of SLNP, including triglycerides [20, 21] and hard fat waxes [22, 23]. Therefore, the choice of emulsifier and co-emulsifier is essential in oral delivery because of the method of administration [24].

Several research groups have explored the influence of lipid type on the final particle size of SLNP dispersions generated [20-25]. The ultimate size of the SLNP dispersions was shown to be affected by factors such as lipid crystallization velocity, lipid hydrophilicity, and the impact of the lipid's self-emulsifying capabilities on the form of the lipid crystals [25].

This study evaluated physicochemical drug characteristics such as solubility in different pH buffers, partition coefficient, melting point, and physical description (such as colour, odour, and physical form) of  $\alpha$ -mangostin. Along with physicochemical characteristics drug was evaluated for its purity by FT-IR (Fourier transform infrared) and DSC (Differential scanning calorimetry) thermograms. Physicochemical characterization of excipients and their compatibility in SLNP formulation is crucial as these parameters influence the stability and quality of the formulated SLNP. Active and excipients were tested for their identity by DSC and FTIR analysis in this study. Any incompatibility between the lipids and the actives was evaluated by conducting compatibility studies for one month at different temperature and humidity conditions. As selecting suitable excipients are essential for any formulation, particularly in oral and parenteral administration, excipients that are GRAS listed are preferred for carrying out the study. After evaluating the physicochemical characteristics of both excipients and drugs, it is essential to select suitable formulation components to formulate SLNP. Right excipients in the right combination are very critical as these parameters influence many factors associated with the formulated SLNP. Screening additives and the technology for a drug like  $\alpha$ -mangostin with very low oral bioavailability is even more critical. Characteristics of solid lipid nanoparticles such as entrapment efficiency, mean particle size, zeta potential and drug loading are dependent on the formulation with suitable excipients and combination. Hence, excipients screening and establishing their ratios in the final formulation is crucial for the formulated SLNP. Ingredients such as solid lipids, emulsifiers, cryoprotectants, the ratio of active: lipid was screened before formulating an optimized SLNP. Solid lipids such as glyceryl monostearate, Compritol ATO 888, Stearic acid and Precirol ATO 5 were initially screened for their solubility of  $\alpha$ -mangostin. Then emulsifier screening is carried out for Methocel K100M, Poloxamer 188, Poloxamer 407 and Tween-80 emulsifiers for particle size and PDI (poly dispersibility index). Screening of saccharides such as Trehalose, Maltose, Mannitol, and Sorbitol as cryoprotectants were done based on particle size and PDI. Finally, the ratio of lipids, emulsifier and co-emulsifier, estimation of cryoprotectant and ratio of lipid: drug was evaluated for the preparation of optimized formulation of solid lipid nanoparticles.

## 2. RESULTS AND DISCUSSION

### RESULTS

#### 2.1 Physico-chemical properties characterization

Physico-chemical properties were evaluated for the  $\alpha$ -mangostin drug. The evaluated parameters are given below in Table 1.

**Table 1: Physico-chemical parameters of  $\alpha$ -Mangostin**

Physico-chemical parameters		$\alpha$ -Mangostin
Melting point	Colour	Faint yellowish brown colour
	Odour	Characteristic herbal odour
	Physical state	Crystalline powder
	Capillary method	181.5°C
	Differentiation scanning calorimeter	Sharp endotherm at 195.98°C

### 2.1.1 Partition coefficient

Drugs with partition coefficient value greater than "1" are considered to be hydrophobic and the value less than "1" is considered to be lipophobic. The values of partition coefficient were given in Table 2

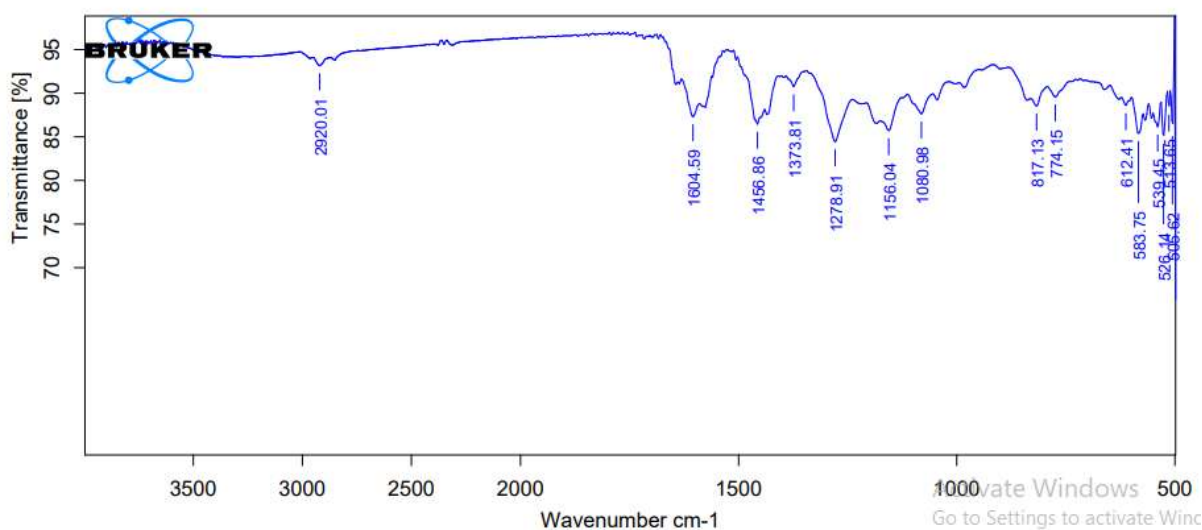
**Table 2:  $\alpha$ -mangostin partition coefficient results**

Ratio of Octanol: Water	Drug concentration in Octanol (mg/mL)	Drug concentration in Water (mg/mL)	$P_{O/W}$	Log P
1:1	1.084	0.473	2.29	0.359 $\pm$ 0.007

### 2.1.2 Identification test

#### Fourier transform infrared spectrophotometry

Figure 1 show the FT-IR spectra of  $\alpha$ -mangostin obtained using the potassium disc technique. The results were compared to standard spectra, and the corresponding spectrum values are listed below. The absorption peaks of  $\alpha$ -mangostin are 2920  $\text{cm}^{-1}$ , 1604  $\text{cm}^{-1}$ , 1456  $\text{cm}^{-1}$ , 1373  $\text{cm}^{-1}$ , 1278  $\text{cm}^{-1}$ , 1080  $\text{cm}^{-1}$ , 774  $\text{cm}^{-1}$ , and 612  $\text{cm}^{-1}$  are  $-\text{CH}_2$  stretching vibration,  $\text{C}=\text{C}$  un-conjugated stretching vibration,  $\text{CH}_2$  bending,  $\text{CH}_3$  bending,  $\text{C}-\text{O}$  stretching vibration,  $\text{C}-\text{OH}$  stretching,  $-(\text{CH}_2)_n$ , and  $-\text{HC}=\text{CH}-$  bending. The drug sample



is validated by the absorption peaks of the various groups with very minimal variance.

**Figure 1: FT-IR Spectra of  $\alpha$ -mangostin**

### Differential scanning calorimetry

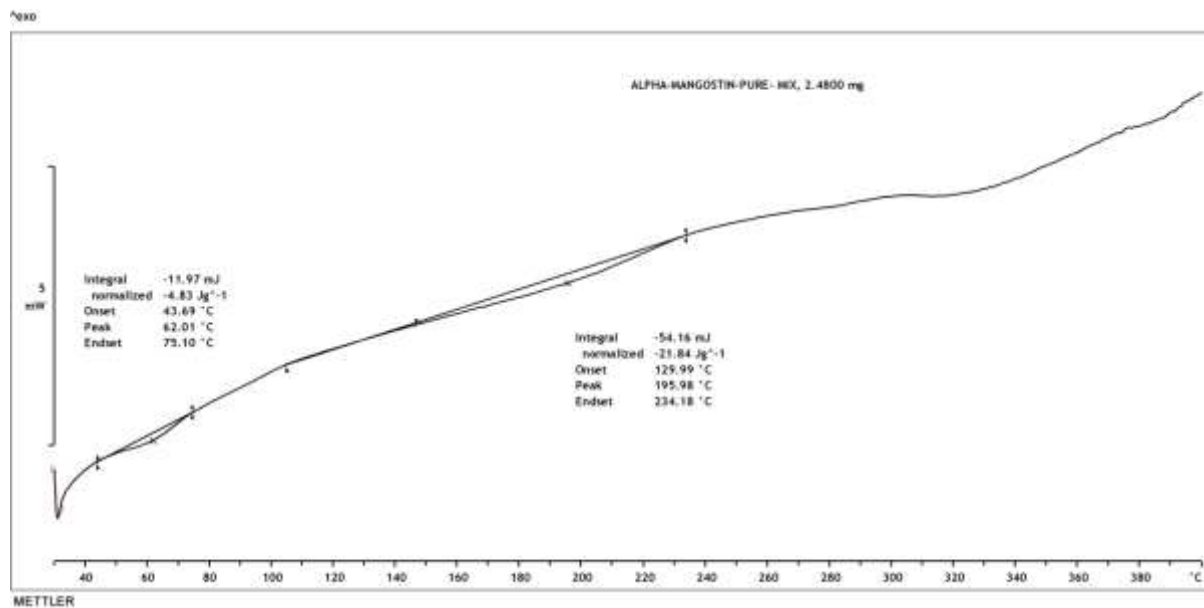
To evaluate melting point of  $\alpha$ -mangostin DSC studies were carried out within the temperature ranges between 30 and 300°C. The observed melting point was found to be 195.98°C (Figure 2).

**Figure 2: DSC thermogram of  $\alpha$ -mangostin**

### Drug–lipid/emulsifier interaction studies

To determine the melting point of  $\alpha$ -mangostin, DSC experiments were conducted at temperatures ranging from 30 to 300°C. 195.98°C was discovered to be the melting point. Four weeks were spent evaluating the physicochemical interactions between the medication and the additives. When comparing the test group to the reference group, no physical alterations were noted. DSC experiments for pure drug, lipids, and a physical combination of drug and lipids revealed no chemical interactions.  $\alpha$ -mangostin, Stearic acid, and Precirol ATO5 have melting points of 195.98°C, 58.97°C, and 73.42°C, respectively (Table 3). The findings indicate that the additions are compatible with the active ingredient.

**Table 3: Pure ingredients and physical mixtures DSC study details**



Pure ingredients and physical mixtures DSC study details		Melting point	Reference
$\alpha$ -mangostin	Reported	180-185°C	[39]
	Experimental	195.98°C	
Stearic acid	Reported	69-72°C	[40]
	Experimental	50.71°C	
Precirol ATO5	Reported	50-60°C	[41]
	Experimental	62.5°C	
$\alpha$ -mangostin+stearic acid+ Precirol ATO5	$\alpha$ -mangostin	190.86°C	
	Stearic acid	58.75°C	
	Precirol ATO5	71.56°C	

### Determination of drug solubility

It is essential to conduct a solubility study for 10-12 hours without producing degradants to achieve equilibrium solubility of the drug. For best results, a phase-solubility investigation should be carried out within a specific time frame. The saturation solubility of the drug was evaluated in different pH buffers and distilled water, and samples were analyzed at 317nm by HPLC. Compared to other pH buffers,  $\alpha$ -mangostin has a high solubility in 7.5 pH PBS buffers. The results are given in Table 4 below.

**Table 4: Solubility data of  $\alpha$ -mangostin in different pH buffers**

pH values and buffer solvents used	Drug solubility (mg/mL)
1.2 $\pm$ 0.01 (0.1N HCL buffer)	0.3072 $\pm$ 0.076
6.80 $\pm$ 0.01 (PBS buffer)	0.4576 $\pm$ 0.087
7.50 $\pm$ 0.01 (PBS buffer)	0.5784 $\pm$ 0.099
7.01 $\pm$ 0.01 (Distilled water)	0.4892 $\pm$ 0.071

## 2.2 Process optimization trials

### 2.2.1 Optimization of homogenization Speed

Homogenization at 15,000 rpm showed the lowest particle size (243.6 nm) and the highest entrapment efficiency (78.41%) compared to the other two homogenization speeds. Hence, homogenization at 15,000 rpm for 30 minutes was optimized for further experiments by hot melt homogenization followed by ultrasonication. The results of particle size and PDI are given in Table 5 below.

**Table 5: Homogenization speed (HS) effect on particle size and entrapment efficiency of solid lipid nanoparticle of  $\alpha$ -mangostin**

Formulation	Homogenization speed	Particle size (nm) $\pm$ SD	EE(%) $\pm$ SD
HS-1	5,000 rpm	321 $\pm$ 11.16	67.12 $\pm$ 1.95
HS-2	10,000 rpm	286.45 $\pm$ 12.39	76.26 $\pm$ 2.08
HS-3	15,000 rpm	243.6 $\pm$ 13.14	78.41 $\pm$ 1.46

### 2.2.2 Optimization of ultrasonication time

Even though the particle size and PDI values were a little larger when ultrasonication was carried out at 9 minutes compared to 6 minutes, further studies were carried out at 6 minutes to avoid metal contamination [36]. The results of particle size and PDI are given in Table 6 below.

**Table 6: Ultrasonication (US) time effect on particle size of solid lipid nanoparticle of  $\alpha$ -mangostin**

Formulation	Ultrasonication time	Particle size (nm) $\pm$ SD	PDI
US-1	3 minutes	273 $\pm$ 18.11	0.478
US-2	6 minutes	245.76 $\pm$ 11.61	0.396
US-3	9 minutes	241.98 $\pm$ 16.32	0.361

## 2.3 Selection of formulation components

### 2.3.1 Lipid screening

The percent entrapment efficiency of a drug is directly influenced by its solubility and partitioning in lipid [37]. Table 7 summarizes the results of the drug partitioning in lipids. When compared to other lipids, Stearic acid had superior solubility and partition. For further formation of solid lipid nanoparticles, the high partition coefficient of  $\alpha$ -mangostin in Precirol ATO5 and Stearic acid was used.

**Table 7: Partition behavior of  $\alpha$ -mangostin in different solid lipids**

S. NO	Solid lipid	HLB value	Partitioning concentration of $\alpha$ -mangostin
1	Compritol ATO 888	2	7.25 $\pm$ 0.11
2	<b>Precirol ATO5</b>	<b>2</b>	<b>9.58 <math>\pm</math> 0.21</b>
3	Glyceryl mono stearate	3.8	8.41 $\pm$ 0.37
4	<b>Stearic acid</b>	<b>15</b>	<b>9.68 <math>\pm</math> 0.17</b>

### 2.3.2 Surfactant screening

For preliminary screening, four surfactants were chosen. The particle size of lipid nanoparticles was measured using a 1:2 ratio of surfactant: lipid. The results revealed that poloxamer-407 had the smallest particle size and a unimodal size distribution. Other surfactants have a larger particle size distribution and a multi-modal size distribution. As a result, poloxamer-407 will be employed for additional formulation optimization investigations in this study. Table 8 shows the findings of particle size and distribution. In comparison to particles generated by poloxamer-407, the mean particle size distributions are much greater. Thus, despite having a bimodal size distribution, poloxamer-407 was chosen as a surfactant and sodium taurocholate was chosen as a co-surfactant, based on their higher HLB values, which are required to emulsify a lipid mixture (Stearic acid and Precirol ATO5) and generate sufficient negative charge over the SLNP. The stabilizers might precipitate and adsorb on the surface of solid lipid nanoparticles, forming a steric barrier that would prevent agglomeration and particle growth.

**Table 8: Surfactant screening for formulation of solid lipid nanoparticles**

S. No	Surfactant	HLB	Mean particle size(nm)	PDI
1	Methocel K100M	–	422 $\pm$ 21.16	0.624
2	Poloxamer188	29	240.6 $\pm$ 11.18	0.435
3	<b>Poloxamer 407</b>	<b>18</b>	<b>185.2<math>\pm</math>12.96</b>	<b>0.212</b>
4	Tween80	15	395.4 $\pm$ 16.82	0.397

### 2.3.3 Cryoprotectant screening

Sugars including trehalose, maltose, mannitol, and sorbitol (5 percent w/v) were tested as cryoprotectants during the lyophilization process to keep SLNP from aggregation together [38]. The cryoprotected SLNP were lyophilized and ultrasonically dispersed in distilled water before being analyzed for mean particle size. In comparison to the original formulation, the mean particle size of all lyophilized samples is 1.043–1.73 times larger. Sorbitol has a multimodal size distribution with a mean particle size of 418.6 nm. Trehalose, maltose, and mannitol, on the other hand, had submicron mean particle sizes of about 636.7 nm, 553.6 nm, and 382.4 nm, respectively. The mean particle size of SLNP was larger with Trehalose (Trehalose > Maltose > sorbitol > mannitol > without cryoprotectant) and lower with no cryoprotectant. Despite the fact that the mean particle size of the SLNP increased from 366.3 nm (without cryoprotectant) to 382.4 nm (with mannitol as a cryoprotectant), mannitol was chosen for further studies as the most effective cryoprotectant among the compounds tested because it did not show a significant variation in mean particle size. The results were given in Table 9 below.

**Table 9: Particle size and PDI values of SLNP with and without cryoprotectants.**

S. No	Cryoprotectants	Mean Particle size(nm)	PDI
1	Trehalose	636.7 $\pm$ 32.17	0.352
2	Maltose	553.6 $\pm$ 29.87	0.463
3	<b>Mannitol</b>	<b>382.4<math>\pm</math>18.19</b>	<b>0.531</b>
4	Sorbitol	418.6 $\pm$ 13.21	0.644



5	Without Cryoprotectant	366.3 $\pm$ 15.76	0.474
---	------------------------	-------------------	-------

#### 2.3.4 Estimation of lipid-lipid ratio

Initially, preliminary experiments were performed to determine the significant factors and the suitable range of elements necessary for the formulation of  $\alpha$ -mangostin loaded SLNP with desired characteristics. The purpose of the study was to explore the outcome of particle size on the combination of Stearic acid and Precirol ATO5. These lipids were chosen based on a higher partition coefficient of the drug. The SLNP been prepared with the combination of Stearic acid and Precirol ATO5 in different concentrations (0.25-1g) and were analyzed for particle size and PDI. The combination of Stearic acid (0.40g) and Precirol ATO5 (0.60g) showed the smallest mean particle size and PDI that is 357.2nm and 0.351, respectively, with monomodal size distribution (Table 10). Therefore, the concentration mentioned above was further selected for the encapsulation of drug.

**Table 10: Estimation of lipid-lipid (LL) ratio on the basis of particle size of SLNP.**

Formulation	Stearic Acid		Precirol ATO5		Mean Particle size (nm)	PDI
	(%)	(g)	(%)	(g)		
LL-1	1	1	0	0	605.2 $\pm$ 22.18	0.649
LL-2	0	0	1	1	583.5 $\pm$ 16.78	0.498
LL-3	1	0.5	1	0.5	440.5 $\pm$ 18.49	0.456
LL-4	2	0.67	1	0.33	456.4 $\pm$ 12.67	0.557
LL-5	3	0.75	1	0.25	467.7 $\pm$ 23.15	0.714
<b>LL-6</b>	<b>2</b>	<b>0.4</b>	<b>3</b>	<b>0.6</b>	<b>357.2<math>\pm</math>14.92</b>	<b>0.351</b>
LL-7	3	0.6	2	0.4	440.5 $\pm$ 14.34	0.461
LL-8	1	0.25	3	0.75	398.3 $\pm$ 15.67	0.706
LL-9	1	0.33	2	0.67	472.3 $\pm$ 13.21	0.581

#### 2.3.5 Estimation of the drug-lipid ratio

The effects of different drug-lipid ratios (1:1–1:5) on particle size and encapsulation efficiency of SLNP were investigated (Table 11). It was discovered that increasing the concentration of lipids ratios improved particle size and encapsulation efficiency up to 1:2 drug-lipids ratio, however after 1:2 lipids ratios, particle size raises with no significant improvement in encapsulation efficiency. The micro-emulsion droplets are surrounded by an interfacial coating made up of surfactant and co-surfactant. A micro-emulsion has three phases: an oil phase, a water phase, and an interphase. The concentration of three phases, which impacts particle size and encapsulation effectiveness, was the most important issue while making SLNP using the micro-emulsion process. After increasing the lipid concentration from 1:1 to 1:5, a considerable increase in particle size was seen, but no significant improvement in encapsulation efficiency was observed after increasing the drug-lipid ratio to 1:2 while maintaining the surfactant, co-surfactant, and co-solvent unchanged. Encapsulation efficiency rises up to 79.4% at a 1:2 drug-lipid ratio; however, increasing the drug-lipid ratio did not improve encapsulation efficiency. This was owing to the lipid matrix becoming saturated and the greater loading amount.

**Table 11: Estimation of drug-Solid lipid (DSL) ratio based on particle size and encapsulation efficiency**

Formulation	Drug-solid lipid ratio	Poloxamer-407	Sodium Taurocholate	Particle size (nm) $\pm$ SD	PDI	EE (%) $\pm$ SD
DSL-1	1:1	0.5	0.5	185.5 $\pm$ 14	0.271	57.5 $\pm$ 1.87
<b>DSL-2</b>	<b>1:2</b>	<b>0.5</b>	<b>0.5</b>	<b>192.5<math>\pm</math> 73</b>	<b>0.293</b>	<b>79.4<math>\pm</math>2.11</b>
DSL-3	1:3	0.5	0.5	271.9 $\pm$ 80	0.411	78.7 $\pm$ 2.18

DSL-4	1:4	0.5	0.5	314.8	0.428	77.4 $\pm$ 1.93
DSL-5	1:5	0.5	0.5	391.1 $\pm$ 28	0.745	79.2 $\pm$ 2.24

### 2.3.6 Estimation of surfactant and co-surfactant ratio

Surfactant and co-surfactant concentrations of poloxamer-407 and sodium taurocholate (STC) were adjusted from 0.25 to 0.75 percent (w/w). The impact of stabilizer concentration was also investigated, and it was shown that the equal ratio of surfactant and co-surfactant (0.5:0.5) is necessary to stabilize the chosen lipids. The SUR-5 formulation has the smallest particle size (191.4 nm). Formulations 2,4,6 and 9 showed PDI greater than 0.50 and formulations 1,2,4,5 and 7 showed zeta potential value greater than -30mV. The SUR-5 was chosen as the best of all the formulations which shown lowest particle size (191.4nm), good zeta potential (-32.17mV) and less than 0.50 PDI (0.379). The values were given in Table 12 below.

**Table 12: Surfactant and co-surfactant (SUR) concentration with their respective zeta potential and particle size**

Formulation Number	Poloxamer-407		STC		Zeta Potential (mV)	Particle size (nm)	PDI
	(%)	(g)	(%)	(g)			
SUR-1	0.25	0.25	0.25	0.25	- 40.05	292.5 $\pm$ 12.16	0.137
SUR-2	0.50	0.50	0.25	0.25	- 32.17	327.1 $\pm$ 14.71	0.676
SUR-3	0.75	0.75	0.25	0.25	- 24.18	348.3 $\pm$ 07.61	0.417
SUR-4	0.25	0.25	0.50	0.50	- 37.31	294.9 $\pm$ 18.19	0.668
<b>SUR-5</b>	<b>0.50</b>	<b>0.50</b>	<b>0.50</b>	<b>0.50</b>	<b>- 32.17</b>	<b>191.4<math>\pm</math>11.31</b>	<b>0.379</b>
SUR-6	0.75	0.75	0.50	0.50	- 24.60	274.4 $\pm$ 16.28	0.578
SUR-7	0.25	0.25	0.75	0.75	- 40.27	216.7 $\pm$ 16.17	0.484
SUR-8	0.50	0.50	0.75	0.75	- 29.58	373.2 $\pm$ 15.47	0.460
SUR-9	0.75	0.75	0.75	0.75	- 17.16	359.7 $\pm$ 13.82	0.574

### 2.3.7 Estimation of mannitol concentration

Mannitol acts as a cryoprotectant, keeping away SLNP from aggregating during lyophilization and assisting with SLNP reconstitution right before administration. For optimization, mannitol concentrations ranging from 2.5 percent to 7.5 percent (w/w) were tested. The average particle size and size distribution were found to be closely related to the amount of mannitol used. When the quantity of mannitol in the formulations M-1 and M-2 is increased, there is significant change in mean particle size or polydispersity index (Table 13). The size distribution of formulation M-1 was bimodal, whereas the size distribution of formulation M-2 was monomodal. The formulation M-2 with 5 percent (w/w) mannitol had the mean particle size (283 nm) and a polydispersity index of 0.256, indicating a monomodal size distribution.

**Table 13: Mannitol (M) concentration and their respective particle size and polydispersity index values.**

Mannitol concentration	% W/V Mannitol	Average particle size (nm $\pm$ SD)	PDI
M-1	2.5	242.1 $\pm$ 24.32	0.335
<b>M-2</b>	<b>5.0</b>	<b>283.0<math>\pm</math>15.41</b>	<b>0.256</b>
M-3	7.5	320.0 $\pm$ 14.67	0.389



## DISCUSSION

Formulating a stable SLNP with high entrapment efficiency, zeta potential, and smaller particle size is possible when there are proper excipients in a suitable combination. Screening process variables and excipients are critical to achieving the right objective when formulating a nanoparticle. A high concentration of excipients not only decreases the concentration of drugs available in the formulation but also impacts the efficacy of the formulation.

For example, screening one or two excipients by trial and error yields products that may not be reproducible and economical. The effect of one variable in the presence of other variables at one particular ratio is significant, particularly in formulating a SLNP. However, one factor at a time does not provide any relation between the combinations of excipients. Hence, a series of screening steps will yield data that can interpret the relationship between the ratios and give a stable formulation. This study aims to maximize the concentration of drugs available in nanoparticles by minimizing the concentration of excipients by screening every excipient in its particular form and in combination, which will give a clear idea of different processes and excipient variables affecting the desired objective of formulating stable SLNP.

Followed a series of steps to screen excipients for the formulation of SLNP with high entrapment efficiency, zeta potential, and smaller particle size and PDI.

Initially, ethanolic extract of  $\alpha$ -mangostin physicochemical characteristics was evaluated. The melting point of  $\alpha$ -mangostin by the capillary method and the DSC studies were found to be similar with marginal differences. Partition studies confirms lipophilic nature of active moiety. Found higher partitioning behavior in the octanol phase than in the water phase. FT-IR studies were performed for ethanolic extract of  $\alpha$ -mangostin and compared with standard spectra of  $\alpha$ -mangostin. Observed no differences in characteristic peaks when comparing the spectra of ethanolic extract of  $\alpha$ -mangostin with pure  $\alpha$ -mangostin. Performed solubility across the pH range of 1.2 to 7.5. Even though the solubility of  $\alpha$ -mangostin is high in a 7.5 pH buffer, there is no significant difference in solubility across the pH range, which confirms that drug solubility is pH-independent.

Process and excipient variables were screened simultaneously in a series of steps.

Screened solid lipids such as Stearic acid and Precirol ATO5 as the combination of lipids will give a better quality of SLNP.

As the process adopted for the preparation of SLNP is hot melt homogenization followed by ultrasonication optimization of homogenization cycles and ultrasonication time is necessary. Homogenization at 15,000 rpm yielded particles with high entrapment efficiency and smaller particle size. Hence homogenization cycle is optimized at 15,000 rpm for further screening of process and excipient variables.

Keeping homogenization cycles at 15,000 rpm, further ultrasonication screening at 3, 6, and 9 minutes. Even though 9 minutes of sonication yielded a smaller particle size, PDI optimized 6 minutes of sonication time to avoid metal contamination associated with ultrasonication.

Screened Poloxamer 407 as a surfactant yielded a smaller particle size and PDI than the other surfactant. Used sodium taurocholate as a co-emulsifier for generating a negative charge on the surface of the lipid nanoparticles.

For lyophilization of formulated solid lipid nanoparticles, used to improve the stability of the formulation. Mannitol was screened as the lyophilizer, yielding a smaller particle size and PDI than other lyophilizers. Individual screening of excipients such as lipids, surfactants, and cryoprotectants; screening of process parameters, homogenization cycle, and sonication time yielded proper excipients and process parameters for the formulation of solid lipid nanoparticles but did not give the idea of a combination of excipients and their interactions. Performed further screening to evaluate the ratio of excipients and their combinations.

Screened the combination of two lipids at different ratios. Combination of the 2: 3 ratio of Stearic acid: Precirol ATO5 yielded particles of smaller particle size and PDI than the other combinations. Hence, 2:3 ratios are the optimized ratio of solid lipids used to formulate solid lipid nanoparticles.

Done Surfactant to co-surfactant screening by keeping the previously optimized concentration of solid lipids (2:3 ratio of Stearic acid: Precirol ATO5) constant. Combination 0.5:0.5 of Poloxamer 407: Sodium taurocholate is the optimized combination ratio for different formulations of solid lipid nanoparticles.

To maximize the concentration of drugs available in the solid lipid nanoparticles, further screening is done by evaluating the ratio of drugs: to lipids. Keeping the ratio of solid lipid (2:3 ratio of Stearic acid: Precirol ATO5) and surfactant: co-surfactant (0.5:0.5) constant. 1:2 ratio of drug: solid lipid is optimized as this ratio yielded particles of smaller size and high entrapment efficiency compared with other ratios. Hence, the 1:2 ratio of Drug: Solid lipid is the optimized combination for further formulation of solid lipid nanoparticles. Finally, lyophilizer concentration is optimized at a 5% w/w ratio of mannitol, yielding particles of smaller size and PDI.

Overall the optimized formulation of solid lipid nanoparticle of  $\alpha$ -mangostin contains a 1:2:0.5:0.5:5 ratio of  $\alpha$ -mangostin: Solid lipid (0.8:1.2 ratio of Stearic acid: Precirol ATO5): Precirol ATO5: Sodium taurocholate: Mannitol. This combination of optimized formulation yielded the smallest particle size and PDI, high entrapment efficiency, and zeta potential. The optimized formulation yielded a particle size of 283nm with a PDI of 0.256. The zeta potential is -36.2Mv, and the entrapment efficiency was 76.29%. The process of hot melt homogenization followed by ultrasonication at 15,000 rpm and 6 minutes of ultrasonication yielded stable solid lipid nanoparticles with minimum particle size and PDI, maximum entrapment efficiency, and zeta potential. The results were tabulated in Table 14.

**Table 14: Optimized formulation of Alpha-mangostin SLNP test results**

Particle Size	PDI	Zeta Potential	Entrapment efficiency
283±11.16nm	0.256	-36.2MV	76.29%

### 3. CONCLUSION

From the screening and further estimations of ingredient ratios, it can be concluded that 1:2 ratio of  $\alpha$ -mangostin: solid lipid (Stearic acid: Precirol ATO5), 2:3 ratio of solid lipids (Stearic acid: Precirol ATO5), 0.5:0.5 ratio of emulsifier: co-emulsifier (Poloxamer 407: STC) and 5% cryoprotectants (mannitol) were screened for carrying out further response surface methodology design experiments.

### 4. MATERIALS AND METHOD

#### MATERIALS

$\alpha$ -mangostin (23% purity) is a gifted sample from Laila Nutraceutical (Andhra Pradesh, India). Solid lipids Stearic acid (Finisar chemicals, Gujarat, India), Compritol ATO-888 and Precirol ATO5 (GattefoscIndiaPvt.Ltd., Mumbai, India) and Glycerylmonostearate(Sigma-Aldrich, New Delhi, India). Surfactant's Poloxamer 188 and 407 were gifted from Mubychemicals (Gujarat, India), Methocel K100M purchased from Dow Wolff cellulosic (Walsroad, Germany) and Tween-80 purchased from Lobachemi (Mumbai, India). Cryoprotectants purchased; Trehalose (Mitushi Biopharma, Ahmedabad, India), Maltose (AB Enterprises, Mumbai, India), Mannitol (Fisher Scientific, Mumbai, India) and Sorbitol (Sisco Research Laboratories Pvt. Ltd., Mumbai, India).

## METHOD

They need many irrefutable important physicochemical parameters to be estimated, learned, and successfully used for active drug substances to formulate an efficient dosage form. These pre-formulation parameters are essential in defining the success of formulation during its developmental events.

### 4.1 Physico-chemical properties

For  $\alpha$ -mangostin, Physico-chemical parameters such as colour, odour, powder physical state, and melting temperature (MP) are measured.

#### 4.1.1 Partition coefficient analysis

The partition coefficient is calculated as the ratio of unionised drugs partitioned into the organic and aqueous phases at equilibrium. The Log P-value of the hydrophobic drug is more than one, whereas the Log P-value of lipophobic pharmaceuticals is smaller than one. The ratio of the drug in unionized form distributed in organic and aqueous phase during its equilibrium is called the partition coefficient of the drug. If the partition coefficient value is greater than "1", it is called a hydrophobic drug. If the value is less than "1", it is called a lipophobic drug.

#### **Po/w = {Concentration of drug in oil phase/Concentration of drug in aqueous phase}**

30mL of each organic (Octanol) and aqueous (Nano-pure water) phase were measured and transferred into a 125mL separating funnel for partition coefficient measurement. To this, 100mg of drug was precisely weighed, and the flask was shaken for 5 hours to attain equilibrium. After 5 hours of shaking, the funnel was laid aside for another 24 hours to ensure optimum drug distribution between the stages. The two layers were separated, diluted, and tested for peak regions in the HPLC equipment after 24 hours of equilibrium.

#### 4.1.2 Identification test

##### *Fourier transform infrared spectrophotometry analysis*

The FT-IR Spectrophotometer is used to determine any physical or chemical interactions between the formulation's components. The preparation of suitable formulations that are stable and successful in their therapeutic response can benefit from FT-IR spectral analysis. FT-IR spectral analysis of potassium bromide pellets with  $\alpha$ -mangostin was carried out in the Bruker FT-IR alpha spectrometer at 4000 to 500  $\text{cm}^{-1}$  range of spectra. About 1-2% of sample was weighed and crushed to a fine powder. The KBr pellets were added and ground together. To minimize scattering losses and absorption band distortions, the sample was very finely ground, as in the Nujol mulling process. The recorded and standard spectra (from the monographs) were compared to see whether there was any compatibility between the formulation's constituents [26].

##### *Differential scanning calorimeter analysis*

DSC analysis was performed with universal V4.5A TA Instruments, and DSC Q-10 V9.9 build. The test was conducted with and without the active component. A sample of 2 mg of each lipid-active and lipid alone (as a control) was sealed in an aluminium pan and assessed at 30-300°C/ nitrogen atmosphere at 60 mL/min with a steady temperature rise of 10°C/minute. Indium is used to standardize instruments.

##### *Drug-lipid/emulsifier interaction studies*

Drug-additives interaction studies were conducted to study the physicochemical features of the active drug moiety in conjunction with additional substances such as additives. Care should be made to choose additives to increase patient compliance, ensure a steady drug release rate, improve bioavailability, and preserve the active component from decomposition. As a result, one-month stability experiments were conducted to assess the incompatibility of the formulation's components.

By preserving the samples in glass ampoules with aluminium closures, the active substances and various solid lipids/ emulsifiers were combined and loaded for stability. Four ampoule sets were constructed and filled for incompatibility testing at three different storage temperatures:

- 5°C for one month
- 25°C with a relative humidity of 60% for one month

- 40°C with a relative humidity of 75% for one month

For one month, the samples were analyzed every week. Then, every week, physical changes were recorded, DSC thermo-grams of the pure drug, lipids chosen for the formulation, and the physical mix of drug-lipid. Studies were carried out in contrast to a control formulation.

#### *Determination of drug solubility*

Because the acidity or basicity of the drug environment affects its degradation, the pH of the solvent affects drug molecule stability. The pH levels in the GIT vary from low to high. As a result, assessing the solubility of the drug in specific environments is crucial to assess its stability. Stability tests were conducted at pH levels ranging from 1.2 to 7.5. Distilled water (pH-7.0), 1.2 pH acid buffers, and 6.8 and 7.5 pH phosphate buffers were used in the experiments. The drug content in each buffer is calculated by making a saturated solution of the drug in each buffer in a conical flask with a capacity of 25 mL. The experiment is conducted in a continuous stirring steady-state (temperature  $37 \pm 0.5^\circ\text{C}$ ) water bath shaker for 48 hours. After 48 hours of stirring, samples were centrifuged at 3,500 rpm for 20 minutes, the supernatant was collected diluted, and drug concentration was determined by HPLC.

### **4.2 Process optimization trials**

#### *4.2.1 Optimization of homogenization Speed*

When it comes to formulating an SLNP, homogenization speed is very critical. We investigated the technique at various homogenization rates while keeping the homogenization duration constant. At three distinct homogenization speeds of 5,000, 10,000, and 15,000 rpm, SLNP were created. Homogenization time is kept constant (30 min) throughout the study. Homogenization cycle is optimized using Alpha-Mangostin: Stearic acid: Precirol ATO5 in 1:1:1 ratio. The assessment parameters for choosing the best homogenization speed were mean particle size and entrapment efficiency.

#### *4.2.2 Optimization of ultrasonication time*

The Q-Sonica sonicator (CL334) was used for the ultrasonication. Ultrasonication was done at 3, 6, and 9 minutes intervals. The ultrasonication time is optimized using Alpha-Mangostin: Stearic acid: Precirol ATO5 in 1:1:1 ratio. The average particle size of the resulting SLNP was measured using the Zetasizer Nano-ZS.

### **4.3 Selection of components for formulation of SLNP**

The choice of additives is crucial. The additives utilized should be GRAS listed, cause no irritation or sensitivity, and be pharmaceutically acceptable. The importance of lipids and surfactants in the preparation of solid lipid nanoparticles cannot be overstated.

#### *4.3.1 Screening of lipids*

In synthesizing solid lipid nanoparticles, factors such as percentage entrapment efficiency (%EE), drug content (%), and drug partition concentration in specific lipids are essential. Partial-glycerides (Compritol ATO 888, Precirol ATO5 & Glycerylmonostearate) and Fatty acids (Stearic acid) were measured in lipids from various categories. Used only lipid and drug without any other excipients in the formulation. Initially, 50mg of the drug and weighed and transferred to 0.5mL of ethanol. The contents were well mixed, and 1g of solid lipids from each category (with melting points above room temperature) was added and homogeneously dispersed. A 5mL of 6.8 pH PBS buffer solution was added to this, and it was shaken for 30 minutes at  $37 \pm 0.5^\circ\text{C}$  on a heated water bath shaker. After thorough maintenance, a 0.22  $\mu\text{m}$  nylon filter separated the aqueous part. The drug content in the aqueous fraction was determined using the HPLC technique.

The partition coefficient can be calculated from the below equation-1:

$$\text{Lipid partition coefficient} = \frac{(\text{Initial drug concentration} - \text{Drug concentration in buffer})}{(\text{Drug concentration in buffer})}$$

#### *4.3.2 Screening of surfactants*

It's critical to choose suitable surfactants to stabilize solid lipid nanoparticles once they've been formulated. Ionic surfactants (cationic and anionic), amphoteric surfactants, and nonionic surfactants are the three types of surfactants accessible. The surface tension of suspensions or dispersions is reduced by these surfactants. When compared to other surfactants, cationic surfactants are more hazardous. The kind of surfactant used to make solid lipid nanoparticles is determined by several criteria, including the mode of administration (oral, parenteral, ETC.), the HLB value of the surfactant, the desired particle size, and its involvement in *in-vivo* lipid breakdown [27]. Surfactants of a nonionic character are preferred for the oral and parenteral delivery routes because they avoid lipid breakdown *in-vivo*. When compared to other surfactants, nonionic surfactants have reduced toxicity and irritation.

Lipase and co-lipase complexes, which promote lipid breakdown, are prevented by the polyethylene oxide chain of these surfactants [28]. The density of these surfactants and their chain length affects the rate of lipid breakdown [29, 30]. As stabilizing agents, nonionic surfactants such as Methocel K100M, Tween-80, Poloxamer 188, and 407 were used, prepared solid lipid nanoparticle with 1:2 ratio of surfactant: lipid and taurocholate sodium in 0.5 per cent (as co-emulsifier) for creating a negative surface charge on the lipid nanoparticle to evaluate the best surfactant suited for the research. Using Alpha-Mangostin: Stearic acid: Precirol ATO5 in 1:1:1 ratio, Homogenization speed at 15,000 rpm and ultrasonication time at 6 minutes screened different surfactants keeping concentration of Sodium taurocholate (co-surfactant) at 0.5 ratio. So the ratio of Active: Lipid (Stearic acid: Precirol ATO5): Surfactant: co-surfactant (Sodium taurocholate)- 1:2(1:1):1:0.5. In addition, the particle size of the generated lipid nanoparticle is used to screen surfactants.

#### 4.3.3 Screening of cryoprotectant

It is critical to lyophilize the emulsion to increase the physical and chemical stability of designed solid lipid nanoparticles. The lyophilization technique tested the physical and chemical stability of produced lipid nanoparticles. Lyophilizations have several drawbacks, such as particle aggregation and instability. This action also destroys the lipid nanoparticle's outermost surfactant layer, reducing the formulation's stability even further. To avoid this issue, various saccharides, such as mannose, trehalose, sorbitol, and others, were utilized as cryoprotectants [31]. During freezing, the particle isolation hypothesis has been proposed as a cryoprotectant stabilization mechanism for nanoparticles. It has been postulated that the sugar isolates individual particles in an unfrozen state, avoiding aggregation during freeze-drying [32]. The replacement hypothesis during dehydration involves the removal of ice and unfrozen water in the stability mechanism of nanoparticles by cryoprotectant [33]. During the drying process, the dehydration mechanism promotes hydrogen bonding between the polar surface of the nanoparticles and the cryoprotectant. As water replacements, they preserved the original structure of nanoparticles. Nanoparticles in their amorphous shape allow for maximum hydrogen bonding with cryoprotectant. As a result, the stabilizer's crystallization can prevent hydrogen bonding from forming [34]. Used 5% w/v concentration of cryoprotectants keeping other excipients constant at Active: Lipid (Stearic acid: Precirol ATO5): Poloxamer 407 (Surfactant): co-surfactant (Sodium taurocholate)- 1:2(1:1):1:0.5 ratio. Sugars such as trehalose, maltose, mannitol, and sorbitol (5 per cent w/v) were tested as cryoprotectants to prevent SLNP aggregation during the lyophilization process. The SLNP were diluted with various cryoprotectant solutions and pre-frozen for 12 hours at  $-20^{\circ}\text{C}$  before being lyophilized for 24 hours at  $-80^{\circ}\text{C}$  in a free-dryer [35].

### 4.4 Analysis Methodology

#### 4.4.1 RP-HPLC Method:

A reverse phase rapid high performance liquid chromatographic method was developed and validated for quantitative estimation of  $\alpha$ -mangostin extracted from solid lipid nanoparticles of  $\alpha$ -mangostin. Alliance e2695 instruments with Empower-3 analysis software with Quaternary gradient pump, autosampler with X-Bridge C<sub>18</sub> Column packed with octadecyl silane with porous 3.5 $\mu\text{m}$  particles, 100X4.6mm dimensions stationary column used for separation of eluents. Acetonitrile and 0.1%v/v ortho phosphoric acid in 65:35 volumes was used as mobile phase at a flow rate of 1mL/min at a wavelength of 317nm by photo diode array detector. Linearity was established within the concentration range of 17.38-260.90  $\mu\text{g}/\text{ml}$  with  $r^2$  value



0.999. Precision was attained with interday and intraday variations with a relative standard deviation of 0.048-0.165% and 0.036-0.182% respectively.

#### 4.4.2 Particle Size, Zeta Potential and Polydispersity Index Analysis

The formulation particle size and zeta potential were measured using a particle size analyzer's dynamic light scattering technique (Malvern Nano ZS90, Malvern, Worcs, UK). All samples were diluted (1:100) in deionized water before analysis. The diluted samples were either injected into a foldable capillary electrophoresis cell for zeta potential measurement or put in disposable cuvettes for size assessment. DLS data were collected at a constant temperature of 25°C and a fixed light incidence angle of 90°.

#### 4.4.3 Drug Entrapment Efficiency

Using the ultrafiltration/centrifugation procedure, separating the free drug from SLNP yielded the drug entrapment efficiency. The samples were diluted in distilled water (1:200) and filtered via centrifugal filters. A multifunction centrifuge at 4,000 rpm for 10 minutes was used to centrifuge the samples. The HPLC analysis set to 317 nm was used to measure the amount of untrapped Alpha-mangostin in the supernatant contained in the centrifuge tube. Below equation-2 was used to compute the percentage of EE:

$$\text{Entrapment efficiency (\%)} = \frac{\{\text{Total drug content in SLNP} - \text{Total free (untrapped) drug}\} \times 100}{\text{Total drug content in SLNP}}$$

#### 4.4.4 Scanning electron microscope

Hitachi S-3700N scanning electron microscope was used to study the morphology of the SLNP (Thane, India). Light sprinkling nanoparticles on a double adhesive carbon tape, which was adhered to an aluminium stub, was used to prepare samples for scanning electron microscopy (SEM). The stub was then coated with gold to a thickness of 200 to 500 microns using a gold sputter module in a high vacuum evaporator under an argon environment. After that, the samples were scanned and photomicrographs were obtained at magnifications of 11,000x. Optimized formulation SEM analysis data presented in Figure 3.

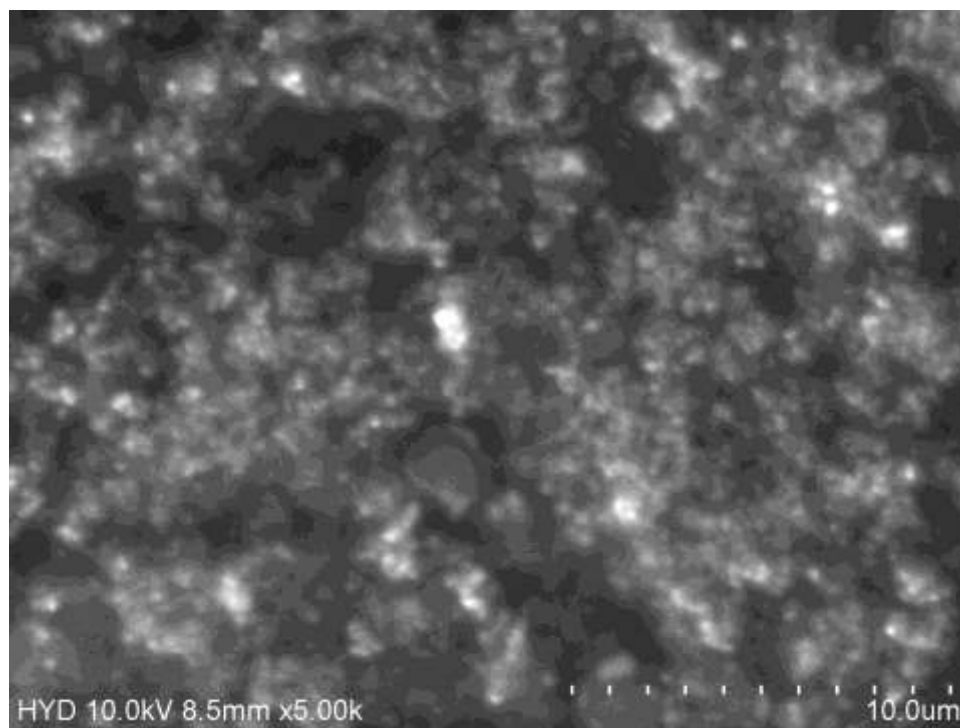


Figure 3: SEM analysis report of optimized formulation



**Acknowledgements:** This work was supported by Laila Nutraceuticals, Vijayawada, Andhra Pradesh, India.

**Author contributions:** Concept –GSN., VNB.; Design – GSN., VNB., GKB.; Supervision – GSN., VNB., DPK.; Resources – ARS., ADP., CHN.; Materials – DPK., ADP., CHN.; Data Collection and/or Processing – GSN, VNB., ARS., RRB.; Analysis and/or Interpretation – VNB., GSN., GKB.; Literature Search – VNB., RRB., GSN.; Writing – VNB., GSN., CHN.; Critical Reviews – GSN., VNB., GKB., ARS., DPK., RRB., ADP., CHN

**Conflict of interest statement:** The authors declared no conflict of interest in the manuscript.

## REFERENCE

- [1] Ji X, Avula B, Khan IA. Quantitative and qualitative determination of six xanthenes in *Garcinia mangostana*L. by LC-PDA and LC-ESI-MS. *J Pharm Biomed Anal* 2007; 43(4): 1270–1276. [\[CrossRef\]](#)
- [2] Obolskiy D, Pischel I, Siriwatanametanon N, Heinrich M. *Garcinia mangostana*L.: A phytochemical and pharmacological review, *Phytother Res* 2009; 23(8): 1047–1065. [\[CrossRef\]](#)
- [3] Pedraza-Chaverri J, Cardenas-Rodriguez N, Orozco-Ibarra M, Perez-Rojas JM. Medicinal properties of mangosteen (*Garcinia mangostana*). *Food Chem Toxicol* 2008; 46(10): 3227–3239. [\[CrossRef\]](#)
- [4] Destandau E, Toribio A, Lafosse M, Pecher V, Lamy C, Andre P. Centrifugal partition chromatography directly interfaced with mass spectrometry for the fast screening and fractionation of major xanthenes in *Garcinia mangostana*. *J Chromatogr A* 2009; 1216(9): 1390–1394. [\[CrossRef\]](#)
- [5] Fang L, Liu Y, Zhuang H, Liu W, Wang X, Huang L. Combined microwave-assisted extraction and high-speed counter-current chromatography for separation and purification of xanthenes from *Garcinia mangostana*. *J Chromatogr B Analyt Technol Biomed Life Sci* 2011; 879(28): 3023– 3027. [\[CrossRef\]](#)
- [6] Chin YW, Kinghorn AD. Structural characterization, biological effects, and synthetic studies on xanthenes from mangosteen (*Garcinia mangostana*), a popular botanical dietary supplement. *Mini Rev Org Chem* 2008; 5(4): 355–364. [\[CrossRef\]](#)
- [7] Pothitirat W, Chomnawang MT, Supabphol R, Gritsanapan W. Free radical scavenging and anti-acne activities of mangosteen fruit rind extracts prepared by different extraction methods. *Pharm Biol* 2010; 48(2): 182–186. [\[CrossRef\]](#)
- [8] Jung HA, Su BN, Keller WJ, Mehta RG, Kinghorn AD. Antioxidant xanthenes from the pericarp of *Garcinia mangostana*(mangosteen). *J Agric Food Chem* 2006; 54(6): 2077–2082. [\[CrossRef\]](#)
- [9] Chen LG, Yang LL, Wang CC. Anti-inflammatory activity of mangosteens from *Garcinia mangostana*. *Food Chem Toxicol* 2008; 46(2): 688–693. [\[CrossRef\]](#)
- [10] Chomnawang MT, Surassmo S, Wongsariya K, Bunyapraphatsara N. Antibacterial activity of Thai medicinal plants against methicillin-resistant *Staphylococcus aureus*. *Fitoterapia* 2009; 80(2): 102–104. [\[CrossRef\]](#)
- [11] Watanapokasin R, Jarinthan F, Jerusalem A, Suksamrarn S, Nakamura Y, Sukseree S, Uthaisang-Tanethpongthamb W, Ratananukul P, Sano T. Potential of xanthenes from tropical fruit mangosteen as anti-cancer agents: Caspase-dependent apoptosis induction in vitro and mice. *Appl Biochem Biotechnol* 2010; 162(4): 1080–1094. [\[CrossRef\]](#)
- [12] Moongkarndi P, Kosem N, Kaslungka S, Luanratana O, Pongpan N, Neungton N. Antiproliferation, antioxidation and induction of apoptosis by *Garcinia mangostana*(mangosteen) on SKBR3 human breast cancer cell line. *J Ethnopharmacol* 2004; 90(1): 161–166. [\[CrossRef\]](#)
- [13] Balunas MJ, Su B, Brueggemeier RW, Kinghorn AD. Xanthenes from the botanical dietary supplement mangosteen (*Garcinia mangostana*) with aromatase inhibitory activity. *J Nat Prod* 2008; 71(7): 1161–1166. [\[CrossRef\]](#)
- [14] Chin YW, Jung HA, Chai H, Keller WJ, Kinghorn AD. Xanthenes with quinone reductase-inducing activity from the fruits of *Garcinia mangostana*(mangosteen). *Phytochemistry* 2008; 69(3): 754–758. [\[CrossRef\]](#)
- [15] Nabandith V, Suzuki M, Morioka T, Kaneshiro T, Kinjo T, Matsumoto K, Akao Y, Iinuma M, Yoshimi N. Inhibitory effects of crude  $\alpha$ -mangostin, a xanthone derivative, on two different categories of colon preneoplastic lesions

induced by 1,2-dimethylhydrazine in the rat. *Asian Pac J Cancer Prev* 2004; 5(4): 433–438.

- [16] Udani JK, Singh BB, Barrett ML, Singh VJ. Evaluation of mangosteen juice blend on biomarkers of inflammation in obese subjects: A pilot, dose-finding study. *Nutr J* 2009; 8: 48. [\[CrossRef\]](#)
- [17] Kondo M, Zhang L, Ji H, Kou Y, Ou B. Bioavailability and antioxidant effects of xanthone-rich mangosteen (*Garcinia mangostana*) product in humans, *J Agric Food Chem* 2009; 57(19): 8788–8792. [\[CrossRef\]](#)
- [18] Li L, Brunner I, Han AR, Hamburger M, Kinghorn AD, Frye R, Butterweck V. Pharmacokinetics of alpha-mangostin in rats after intravenous and oral application, *Mol Nutr Food Res* 2011; 55 (Suppl. 1): S67–S74. [\[CrossRef\]](#)
- [19] Chitchumroonchokchai C, Riedl KM, Suksumrarn S, Clinton SK, Kinghorn AD, Failla ML. Xanthones in mangosteen juice is absorbed and partially conjugated by healthy adults. *J Nutr* 2012; 142(4): 675–680. [\[CrossRef\]](#)
- [20] Heiati H, Tawashi R, Phillips NC. Drug retention and stability of solid lipid nanoparticles containing azidothymidine-palmitate after autoclaving, storage and lyophilization. *J Microencapsul.* 1998;15(2):173–184. [\[CrossRef\]](#)
- [21] Bunjes H, Westesen K, Koch MHJ. Crystallization tendency and polymorphic transitions in triglyceride nanoparticles, *Int J Pharm.* 1996;129(1-2):159-173. [\[CrossRef\]](#)
- [22] Westesen K, Bunjes H, Koch MHJ. Physicochemical characterization of lipid nanoparticles and evaluation of their drug loading and sustained release potential. *J Control Release.* 1997;48(2-3):223-236. [\[CrossRef\]](#)
- [23] Cavalli R, Gasco MR, Morel S. Behaviour of timolol incorporated in lipospheres in the presence of a series of phosphate esters, *STP Pharma Sci.* 1992;2:514-518.
- [24] Mehnert W, Mader K. Solid lipid nanoparticles production, characterization and applications. *Adv Drug Deliv Rev.* 2001;47(2-3): 165-196. [\[CrossRef\]](#)
- [25] Siekmann B, Westesen K. Submicron-sized parenteral carrier systems based on solid lipids. *Pharm Pharmacol Lett.* 1992;1:123-126.
- [26] Mills IIT, Roberson JC, Matchett CC, Simon MJ, Burns MD and Ollis RJ. Instrumental data for drug analysis (IDDA), third edition, CRC Press (Taylor & Francis Group), Boca Raton, London, New York. 2006; Vol-3: 1676–77 (INH), Vol-4: 2710–11 (PYZ) and Vol-4: 2776–77 (RIF).
- [27] Ghasemiyeh P, Mohammadi-Samani S. Solid lipid nanoparticles and nanostructured lipid carriers as novel drug delivery systems: applications, advantages and disadvantages. *Res Pharm Sci.* 2018;13(4):288-303. [\[CrossRef\]](#)
- [28] McClements D, Rao J. Food-grade nanoemulsions: formulation, fabrication, properties, performance, biological fate, and potential toxicity. *Crit Rev FoodSci* 2011; 51(4): 285–30. [\[CrossRef\]](#)
- [29] Olbrich C, Müller RH. Enzymatic degradation of SLN-effect of surfactant and surfactant mixtures. *Int J Pharm* 1999; 180(1): 31–39. [\[CrossRef\]](#)
- [30] Olbrich C, Kayser O, Müller RH. Lipase degradation of Dynasty 114 and 116 solid lipid nanoparticles (SLN)-the effect of surfactants, storage time and crystallinity, *Int J Pharm* 2002a; 237(1): 119–28. [\[CrossRef\]](#)
- [31] Lippacher A, Müller RH, Mäder K. Investigation on the viscoelastic properties of lipid based colloidal drug carriers, *Int J Pharm* 2000; 196(2): 227–30. [\[CrossRef\]](#)
- [32] Amis TM, Renukuntla J, Bolla PK, Clark BA. Selection of Cryoprotectant in Lyophilization of Progesterone-Loaded Stearic Acid Solid Lipid Nanoparticles. *Pharmaceutics.* 2020;12(9):892. [\[CrossRef\]](#)
- [33] Zimmerman E, Müller RH, Mäder K. Influence of different parameters on reconstitution of lyophilized SLN. *Int J Pharm* 2000; 196(2): 211–13. [\[CrossRef\]](#)
- [34] Date PV, Samad A, Devarajan PV. Freeze thaw: a simple approach for prediction of optimal cryoprotectant for freeze drying. *AAPS PharmSciTech.* 2010;11(1):304-13 [\[CrossRef\]](#)
- [35] Ball RL, Bajaj P, Whitehead KA. Achieving long-term stability of lipid nanoparticles: examining the effect of pH, temperature, and lyophilization. *Int J Nanomedicine.* 2016;12:305-315 [\[CrossRef\]](#)
- [36] Kaur I, Ellis LJ, Romer I, Tantra R, Carriere M, Allard S, Mayne-L'Hermite M, Minelli C, Unger W, Potthoff A, Rades S, Valsami-Jones E. Dispersion of Nanomaterials in Aqueous Media: Towards Protocol Optimization. *J Vis Exp.*

2017;(130):56074 [\[CrossRef\]](#)

[37] Arana L, Gallego L, Alkorta I. Incorporation of Antibiotics into Solid Lipid Nanoparticles: A Promising Approach to Reduce Antibiotic Resistance Emergence. *Nanomaterials* (Basel). 2021;11(5):1251. [\[CrossRef\]](#)

[38] Kumar KN, Mallik S, Sarkar K. Role of freeze-drying in the presence of mannitol on the echogenicity of echogenic liposomes. *J Acoust Soc Am*. 2017;142(6):3670. [\[CrossRef\]](#)

[39] National Center for Biotechnology Information (2022). PubChem Compound Summary for CID 5281650, alpha-Mangostin. Retrieved August 24, 2022 from <https://pubchem.ncbi.nlm.nih.gov/compound/alpha-Mangostin>.

[40] National Center for Biotechnology Information (2022). PubChem Compound Summary for CID 5281, Stearic acid. Retrieved August 24, 2022 from <https://pubchem.ncbi.nlm.nih.gov/compound/Stearic-acid>.

[41] Kallakunta VR, Tiwari R, Sarabu S, Bandari S, Repka MA. Effect of formulation and process variables on lipid based sustained release tablets via continuous twin screw granulation: A comparative study. *Eur J Pharm Sci*. 2018 Aug 30;121:126-138. [\[CrossRef\]](#)

This is an open access article which is publicly available on our journal's website under Institutional Repository at <http://dspace.marmara.edu.tr>.